Zootaxa 5165 (3): 346–364
https://www.mapress.com/zt/

Article

ISSN 1175-5326 (print edition)
ZOOTAXA
ISSN 1175-5334 (online edition)

https://doi.org/10.11646/zootaxa.5165.3.2
http://zoobank.org/urn:lsid:zoobank.org:pub:99B81CA6-28B2-4678-84BF-53B6F891B388

A new species of *Ilyobius* Enderlein, 1910 (Megaloptera: Sialidae) from a threatened region in the Mantiqueira Mountain range (Brazil)

GABRIELA CAROLINE MENDES[1,2*], JEANE MARCELLE CAVALCANTE DO NASCIMENTO[1,3], LÍVIA MARIA FUSARI[5], MIREILE REIS DOS SANTOS[6] & NEUSA HAMADA[1,4]

[1]*Coordenação de Biodiversidade-CoBio, Programa de Pós-Graduação em Entomologia (PPGEnt), Instituto Nacional de Pesquisas da Amazônia, Manaus, AM, Brazil.*
[2] *mendaceae@gmail.com; https://orcid.org/0000-0002-5059-2628*
[3] *jeanemarcelle@gmail.com; https://orcid.org/0000-0002-5428-7495*
[4] *nhamada@inpa.gov.br; https://orcid.org/0000-0002-3526-5426*
[5]*Departamento de Hidrobiologia, Universidade Federal de São Carlos (UFSCar), São Carlos, SP, Brazil.*
liviafusari@yahoo.com.br; https://orcid.org/0000-0002-1107-2785
[6]*Instituto Federal de Educação, Ciência e Tecnologia do Sul de Minas Gerais (IFSULDEMINAS), Poços de Caldas, MG, Brazil.*
mireile.santos@ifsuldeminas.edu.br; https://orcid.org/0000-0001-6375-0077
[*]*Corresponding author.* *mendaceae@gmail.com*

Abstract

A new species of *Ilyobius* Enderlein, 1910 (Megaloptera: Sialidae) from the Brazilian Atlantic Forest is described based on male, female, and larva. *Ilyobius erebus* **sp. nov.** is the 11th species in this genus, and the fourth reported in Brazil. In addition, male and female genitalia of *I. hauseri* (Contreras-Ramos, Fiorentin & Urakami, 2005) are redescribed based on the holotype and newly collected specimens at the type locality. Based on the current classification system, *I. erebus* **sp. nov.** is placed in the *I. chilensis* group, which was supported by male and female genital structures. The type locality of the new species is threatened by human impacts, and conservation of its habitat is needed.

Key words: Aquatic insects, alderflies, Neotropical region, Sialinae.

Introduction

Ilyobius Enderlein, 1910 (Megaloptera: Sialidae) was previously considered a junior synonym of *Protosialis* van der Weele, 1909 (Penny, 1981); however, phylogenetic studies have held both genera as valid (Liu *et al*. 2015a). *Ilyobius* includes most of the Neotropical Megaloptera species previously placed in *Protosialis*, except for one species from Cuba that was recently transferred to a monospecific genus, *Caribesialis bifasciata* (Hagen, 1861) (Ardila-Camacho *et al*. 2021). Liu *et al*. (2015a) divided *Ilyobius* species into two groups based on morphological characters of male and female genitalia, namely the *I. chilensis* and *I. mexicanus* groups.

Ilyobius contains 10 extant species (Liu *et al*. 2015a, 2015b; Ardila-Camacho *et al*. 2021), of which three occur in Brazil: *Ilyobius flammatus* (Penny, 1981) in the Amazon Forest, and *Ilyobius hauseri* (Contreras-Ramos, Fiorentin & Urakami, 2005) and *Ilyobius nubilus* (Navás, 1933) in the Atlantic Forest. *Ilyobius hauseri* was described and illustrated based on specimens collected in southern Brazil (Contreras-Ramos *et al*. 2005). In the original description of this species, the male ectoproct was considered to be absent; however, Liu *et al*. (2015a) considered the ectoproct of this species to be the sternite 10 described by Contreras-Ramos *et al*. (2005). After examining the genitalia of the holotype plus additional specimens collected in the type locality of *I. hauseri,* we consider that this controversy occurred due to condition of the genitalia of the type specimen. In the holotype, the ectoproct, gonocoxite and gonostylus 11 complex were internally inverted and covered by tergite 9. We corroborated this fact by examining the male genitalia of specimens collected in the type locality. Also, the presence of gonocoxite 8 in the female genitalia is not mentioned in the original description; however, Liu *et al*. (2015a) considered that this structure was reduced and fused to gonapophysis 8. After analyzing the morphology of the female genitalia of the paratype and the speci-

 Accepted by X.-Y. Liu: 30 Jun. 2022; published: 15 Jul. 2022

mens collected in the type locality, the reduction of gonocoxite 8 mentioned by Liu *et al*. (2015a) was corroborated, but the its fusion with the gonapophysis was not found.

A new species of *Ilyobius* was collected in Morro do Ferro (Poços de Caldas municipality, MG), located in the Mantiqueira mountain range. This region has been undergoing a process of replacement of its natural landscapes as a result of the detrimental actions of the mining industry, real estate speculation (Sardinha *et al*. 2016) and, in recent decades, *Eucalyptus* spp. monoculture (Borges *et al*. 2018).

The objectives of this paper are to describe a new species of *Ilyobius* from Brazil based on male, female and larva and to provide a redescription of the male and female genitalia of *I. hauseri* based on the holotype, paratype and reared specimens collected in its type locality.

Materials and methods

Study area. Poços de Caldas municipality, Morro do Ferro, Minas Gerais (Fig. 1A). The streams where larvae were collected are in a mountain range in the most central portion of the Poços de Caldas Plateau of the Mantiqueira mountain range in the Atlantic Forest domain. The altitudes range from 1250 to 1539 m above sea level, with a mean rainfall of 1700 mm and more than 120 days of rain per year (Chapman *et al*. 1991). The area is characterized by a mosaic of vegetation types including native forests (Atlantic Forest), *campos naturais de altitude* (grasslands in high altitude areas) *matas de galeria* (gallery or riparian forests) and aquatic environments, which are constituted by streams (Moraes *et al*. 2008). Land-use change has altered these landscapes since the last century. The streams (Fig. 1C, D) where larvae of the new species were collected are in a small remnant of natural riparian forest (Fig. 1B) in a landscape dominated by *Eucalyptus* plantations.

Collection and rearing specimens. Malaise and Pennsylvania light traps (Fig. 1C) were installed at the stream's banks; Malaise traps were maintained in the field during six months in 2021; light trap only for three nights. Larvae were collected using a D-net (aquatic net) and maintained alive in plastic vials with a thin layer of water. In the laboratory, the larvae were reared in an acclimatized room (22ºC to 24ºC) and kept isolated in plastic containers with two compartments. One of the compartments, where the larvae were kept and fed, had water and bryophytes, and the second compartment contained wet sand. Because the two compartments were connected, the larvae had free access to the sand compartment to build pupal chambers to complete their development. The containers were kept on a shelf and covered with a piece of dark canvas to reduce the light, simulating the natural environment. Larvae were fed every two days with *Chironomus* (Diptera: Chironomidae) larvae.

Adults and larvae were associated through rearing. Emerged adults were placed together in a terrarium containing sand, plants and tree branches, and they were fed every day with a piece of cotton soaked in a sugar solution.

Taxonomic study. The abdomens of the adults were cut at the level of the third segment and subsequently, the sectioned part was cleared in a solution of 10% potassium hydroxide (KOH) in a hot water bath for about 30 minutes. The cleared structure was then washed with distilled water and 80% ethyl alcohol to remove residues of the alkaline solution. The homology and morphological terminology for the male and female genitalia were based on Liu *et al*. (2016), while the terminology for the external sclerotized structure follows New & Theischinger (1993). The homology and terminology of the wing venation follow Breitkreuz *et al*. (2017). Larval description was based on last-instar larvae and last-instar exuviae. Specimens were fixed in 80% alcohol, and the mouthparts and legs from the exuviae were examined. The morphological terminology for larvae follows New & Theischinger (1993) and Beutel & Friedrich (2008).

Type material of the new species was deposited in Coleção de Invertebrados do Instituto Nacional de Pesquisas da Amazônia; Manaus, Amazonas State, Brazil (INPA) and Museu de Zoologia, Universidade de São Paulo; São Paulo, São Paulo State, Brazil (MZUSP). *Ilyobius hauseri* types to which we had access were represented only by their genitalia (one male and one female) and the original labels. These types belong to Museu de Ciências Naturais, Fundação Zoobotânica do Rio Grande do Sul (MCNZ), Porto Alegre, Rio Grande do Sul State, Brazil.

Multi-focal photographs of the examined specimens were obtained using a Leica M165C stereomicroscope with Leica DFC 420 image-capturing equipment and LED dome lighting for uniform reflection of light on the specimens (Kawada & Buffington 2016). The final images were generated using Digital Leica Application Suite® v.3.7 and Helicon Focus® (6.7.1 Pro) software.

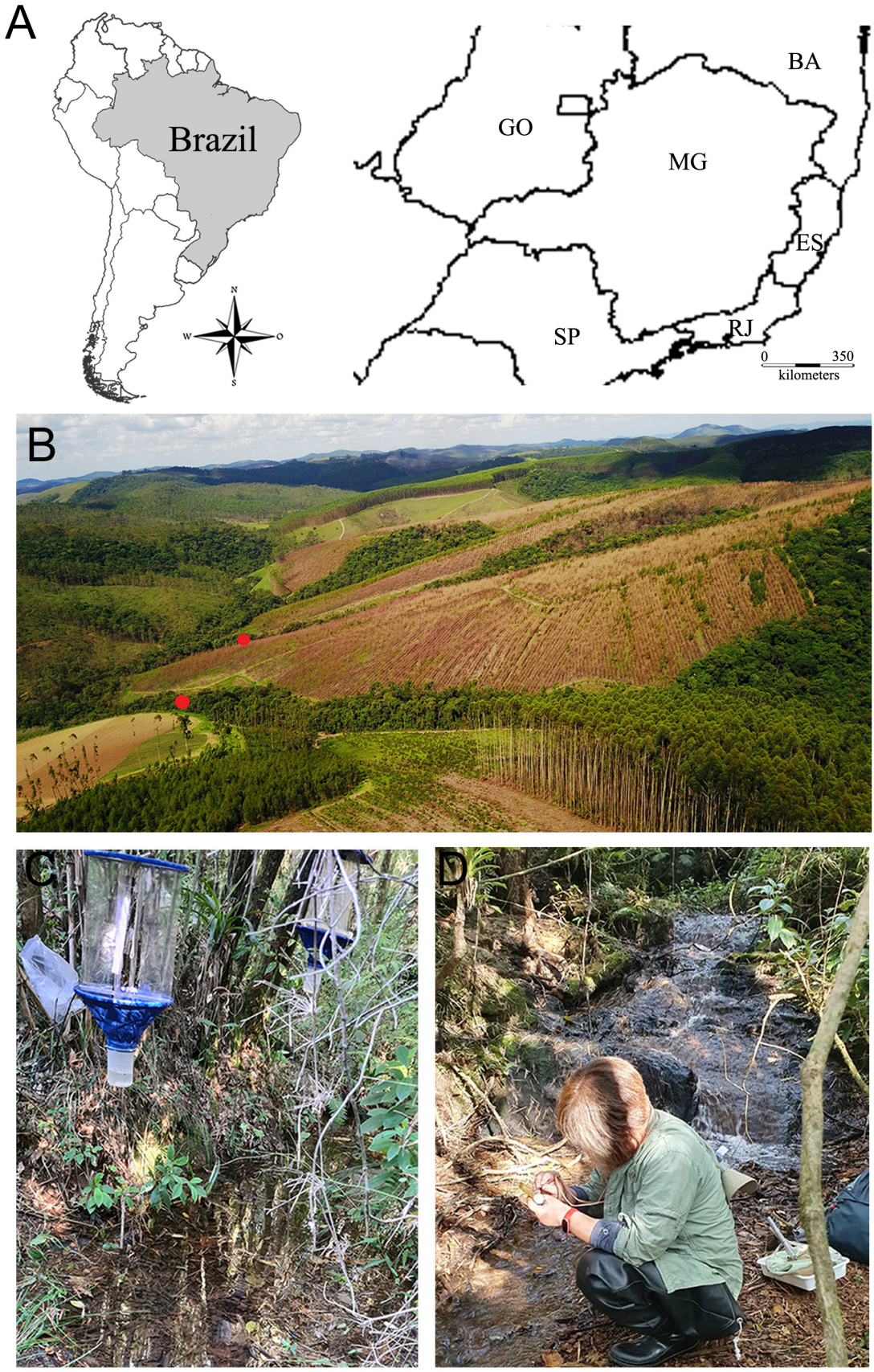

FIGURE 1. (A) Map of South America with detailed area indicating the type locality of *Ilyobius erebus* **sp. nov.** (Megaloptera: Sialidae); (B), (D) general view of the sampled streams. Red spots are localities where *I. erebus* **sp. nov.** was collected; (C) Pennsylvania light traps installed at the stream's banks.

Morphological abbreviations

Abdomen
ect = ectoproct
Gcx 8 = gonocoxite 8
Gcx 9 = gonocoxite 9
Gcx 10 = gonocoxite 10
Gcx 11 = gonocoxite 11
Gph 8 = gonapophysis 8
Gst 9 = gonostylus 9
Gst 11 = gonostylus 11
S7–9 = sternites 7–9
T7–9 = tergites 7–9

Wing venation
A = anal veins
CuA = cubitus anterior
CuP = cubitus posterior
MA = media anterior
MP = media posterior
RA = radius anterior
RP = radius posterior
Sc = subcosta

Results and discussion

Ilyobius erebus sp. nov. Mendes, Nascimento, Fusari & Hamada

(Figs 2–10)

Specimens examined. Holotype: male (pinned), with associated pupal and last instar exuviae in glycerin. Brazil, Minas Gerais State, Poços de Caldas, Morro do Ferro (21°53'33.6''S; 46°33'04.2''W); 16.VI.2021; N. Hamada, L.M. Fusari, J.O. da Silva, M.R. Santos, cols. (INPA).

Paratypes. Same data as holotype: two males: one pinned (INPA), one fixed in 80% alcohol (MZUSP), with pupae and exuviae of the last-instar larvae in glycerin; three females: one pinned (INPA), two fixed in alcohol 80% (one at INPA, one at MZUSP), with pupae and exuviae of the last instar larvae in glycerin; one last-instar larvae (INPA), fixed in 80% alcohol.

Diagnosis. *Ilyobius erebus* **sp. nov.** is distinguished from all other species in the genus by the following characters. Head and pronotum are almost completely blackish, covered with golden setae (Fig. 2A–D). Male sternite 9 is trifurcate, with medial projection longer than lateral ones, in caudal view (Fig. 4C, D). Gonocoxite 9 is robust and subtriangular in lateral view. Ectoproct is rounded in lateral view, with ventral margin fused to gonocoxite 11 (Fig. 4A, B). Gonocoxite 11 is L-shaped in lateral view (Fig. 4A, B), and divided into two sclerites medially connected in caudal view (Fig. 4C, D). Gonostylus 11 is pointed and projected upwards in lateral view (Fig. 4A, B). Female sternite 7 subtriangular in ventral view (Fig. 7C, D), with thumb-shaped projection on distal margin in lateral view (Fig. 7A, B). Gonocoxite 8 is reduced, located beneath sternite 7 (Fig. 7E). Gonapophysis 8 is subrectangular in shape, with anterior margin concave, posterior margin convex, and anterolateral corners falcate in ventral view (Fig. 7C, D). Mature larva head is orange-brown, with darker areas on anterior region (Fig. 8C).

Description. ***Male.*** Body length: mean = 7.17 mm (Standard deviation (SD) ± 0.391, n = 3); Forewing length: mean = 9.18 mm (SD ± 0.839, n = 3); width: mean = 2.54 mm (SD ± 0.361, n = 3); hindwing, length: mean = 8.25 mm (SD ± 1.06, n = 3); width: 2.55–3.10 mm (n = 2).

Head (Fig. 2C, D). Width (at the widest point): mean = 1.64 mm (SD± 0.086, n = 3); length: mean = 1.17 mm (SD ± 0.081, n = 3); region between the posterior margin of the eyes: mean = 1.55 mm (SD ± 0.065, n = 3).

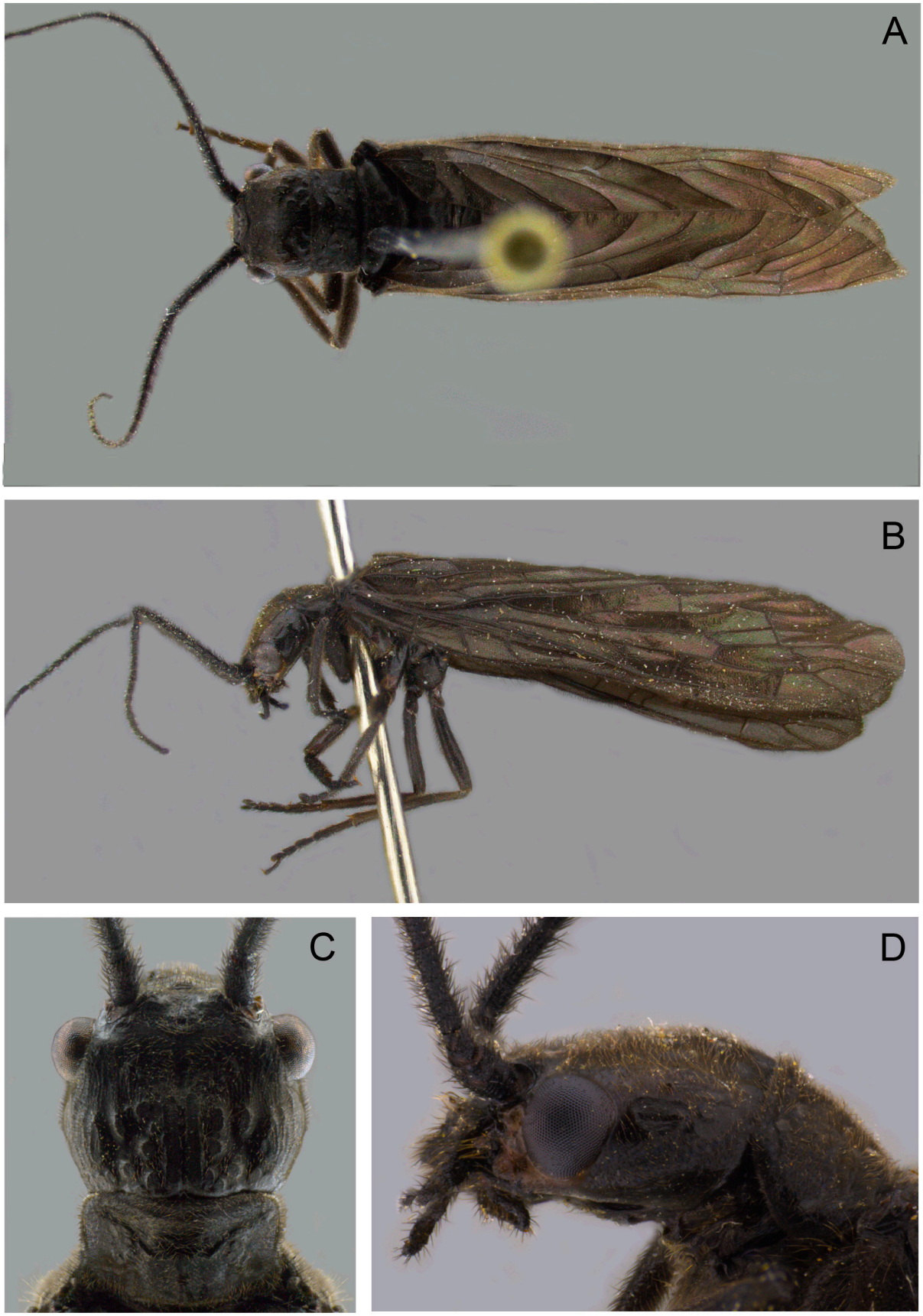

FIGURE 2. *Ilyobius erebus* **sp. nov.**, holotype male. (A) habitus, dorsal; (B) habitus, lateral; (C) head and pronotum, dorsal; (D) head and pronotum, lateral. Scale bars, A, B = 2 mm; C, D = 0.5 mm.

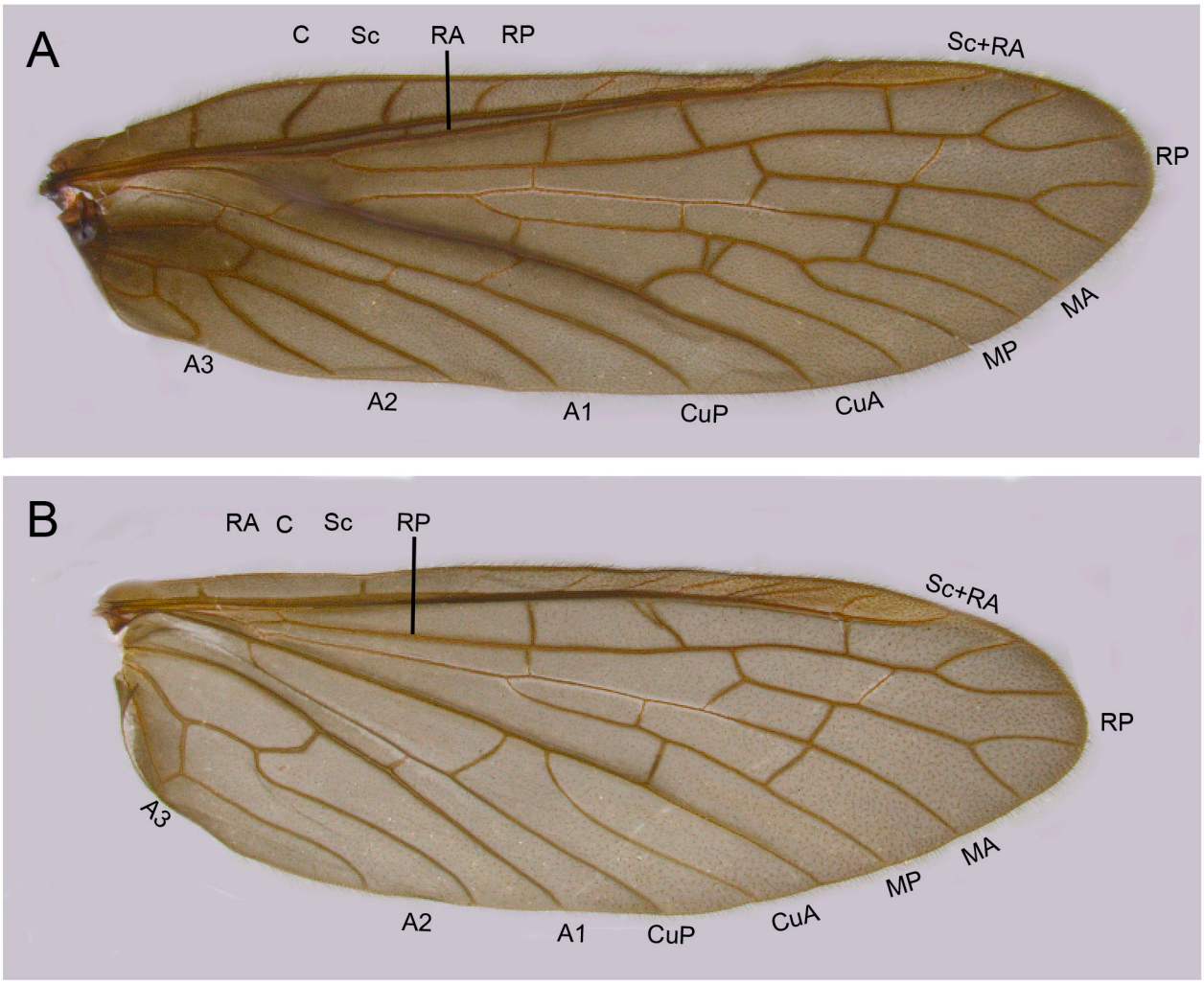

FIGURE 3. *Ilyobius erebus* **sp. nov.**, holotype male, forewing (A) and hindwing (B). Scale bars = 2 mm.

General color blackish, except region of gena, surrounded by dark orange-brown area in lateral view (Fig. 2D); densely covered with golden setae. Scape, pedicel and flagellum blackish, with 30 flagellomeres, densely covered with black setae. Frons with a slight depression between the antennae (Fig. 2C). Posterior region with numerous muscle scars (Fig. 2C). Clypeus and labrum dark brown, densely covered with golden setae; clypeus with median concavity; maxillary and labial palpi dark brown, densely covered with golden and blackish setae (Fig. 2D).

Thorax (Fig. 2A). Pronotum blackish, rectangular; width: mean = 1.54 mm (SD ± 0.097, n = 3); length: mean = 0.75 mm (SD ± 0.063, n = 3), densely covered with golden setae. Meso- and metanotum blackish, subrectangular and densely covered with short, golden setae.

Legs. Dark brown, densely covered with golden setae; fore femur shorter than mid- and hind femur and slightly expanded. Tibial spurs short, yellow. Basitarsi of fore- and midleg short, slightly smaller than second and third tarsomeres together; longer on hind leg, slightly larger than second and third tarsomeres together. Pretarsal claws yellow.

Wings (Fig. 3A, B). Membrane translucent dark brown in alcohol and iridescent blackish *in vivo,* densely covered with golden setae. Veins light brown, pterostigma absent. Forewing: costal area slightly expanded on proximal 1/3 of the wing length, with nine crossveins; radial area with three crossveins; RP with two branches; M bifurcated near mid-length of wing; MA unforked; MP bifurcated near posterior wing margin; mediocubital area with three crossveins; CuA bifurcated near posterior margin; CuP not bifurcated. Intracubital area with a single crossvein. Area between A1 and A2 with a single crossvein; A2 forked before R fork. Area between A2 and A3 with a single crossvein. Hindwing: similar to forewing; costal area undilated, with nine crossveins; radial area with four crossveins; mediocubital area with a single crossvein; MP not bifurcated; anal area expanded (Fig. 3B).

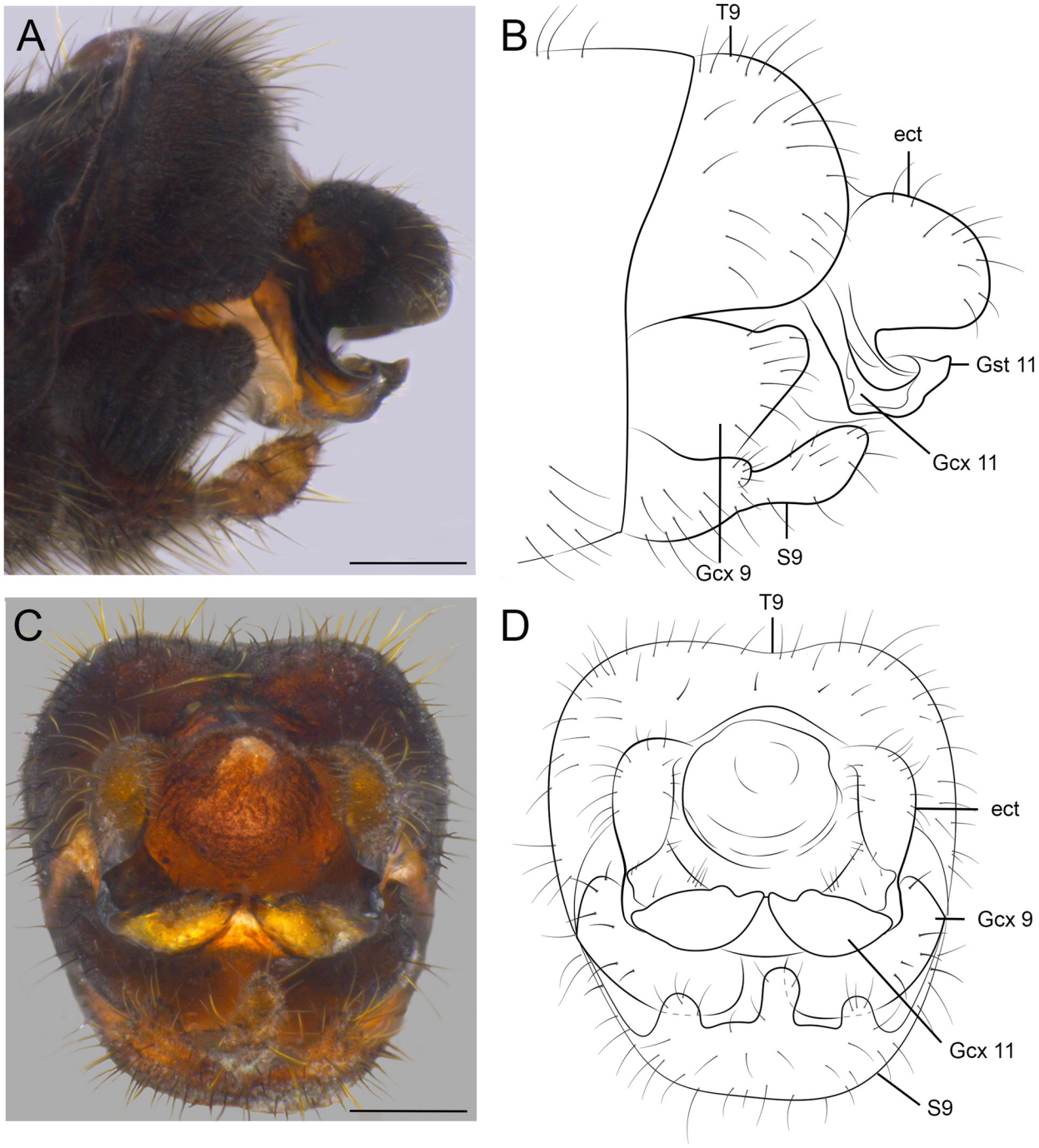

FIGURE 4. *Ilyobius erebus* **sp. nov.**, holotype, male. (A) genitalia, lateral; (B) morphological interpretation of genital sclerites in A; (C) genitalia, caudal; (D) morphological interpretation of genital sclerites in C. Scale bars = 0.2 mm.

Abdomen. Blackish, densely covered with golden setae.

Genitalia (Figs 4A–D; 5A–D; 6A, B). Tergite 9 sclerotized, densely setose; subtriangular with rounded margin in lateral view (Fig. 4A, B); in dorsal view, sub-rectangular; basal margin concave, distal margin convex (Fig. 5A, B). Sternite 9 trifurcate in caudal view, sparsely setose, central projection longer than lateral ones (Fig. 4C, D); in lateral view, medial projection wider medially (Fig. 4A, B); in ventral view, only medial projection is visible, the lateral ones are not visible (Fig. 5C, D). Endophalic sac membranous, eversible, with several fringed thorny setae (Fig. 6A, B). Gonocoxite 9 robust, setose; in lateral view, subtriangular with rounded apex, slightly concave in dorsal region, near the rounded apex (Fig. 4A, B). Anal tubercle membranous. Ectoprocts paired, in lateral view, rounded; dorsal margins convex, ventral margins straight, posteriorly directed, with proximal margins fused to gonocoxite 11

(Fig. 4A, B); in dorsal view, subtriangular, internal margins concave (Fig. 5A, B). Gonocoxite 11 L-shaped in lateral view, distal region pointed at apex and projected upwards, representing gonostylus 11 (Fig. 4A, B); gonocoxite 11 divided into two sclerites that are medially directed and connected by a membranous region in caudal view, setose (Fig. 4C, D); each sclerite with internal margin sinuous.

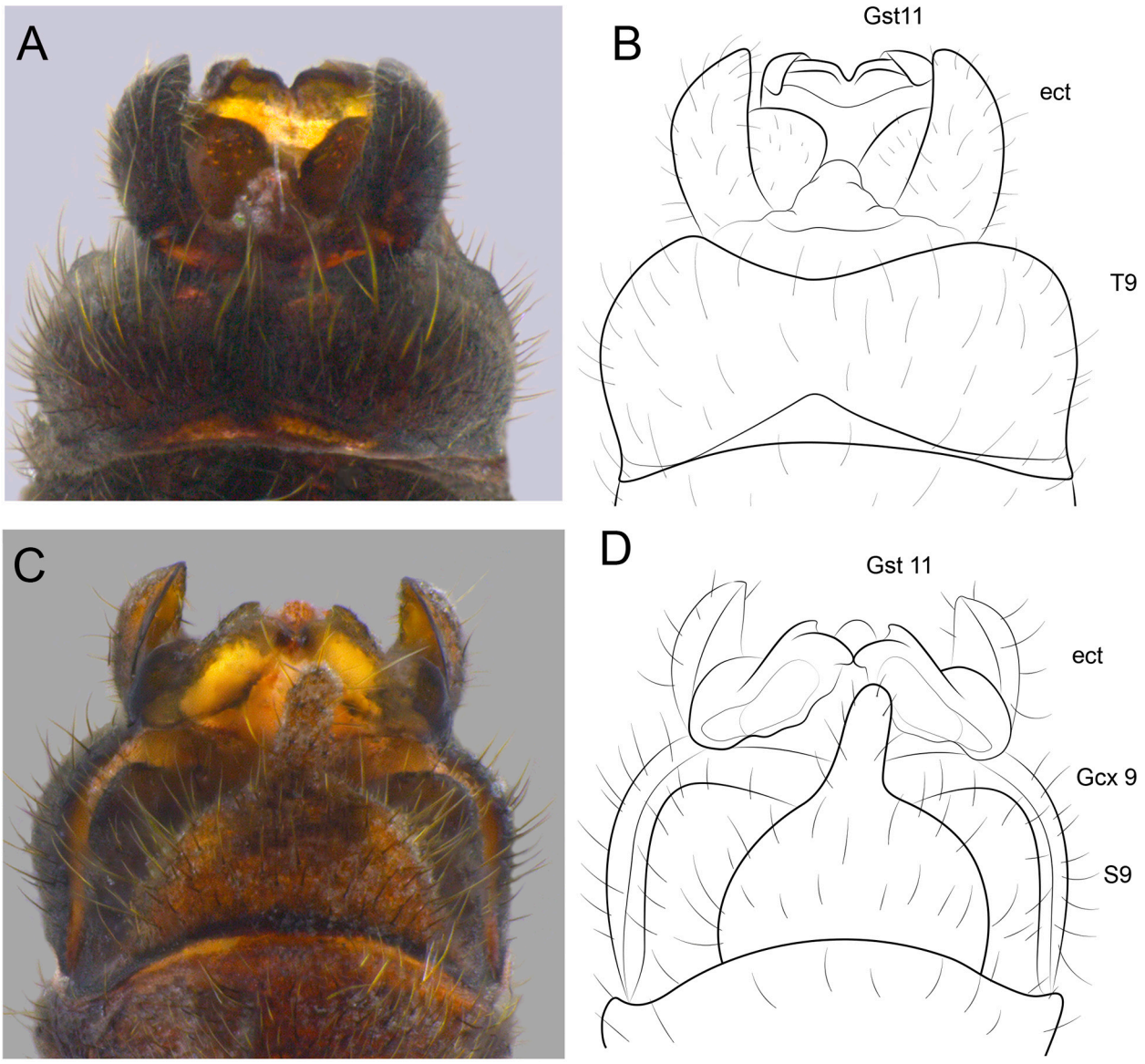

FIGURE 5. *Ilyobius erebus* **sp. nov.**, holotype male. (A) genitalia, dorsal; (B) morphological interpretation of genital sclerites in A; (C) genitalia, ventral; (D) morphological interpretation of genital sclerites in C. Scale bars = 0.2 mm.

Female. Body length: mean = 10.51 mm (SD ± 0.375, n = 3); forewing length: mean = 10.76 mm (SD ± 0.189, n = 3); width: mean = 3.19 mm (SD ± 0.249, n = 3). Hindwing length: mean = 9.25 mm (SD ± 0.573, n = 3); width: mean = 3.53 mm (SD ± 0.166, n = 3).

General coloration and external morphology similar to male.

Head. Width (widest region): mean = 2.10 mm (SD ± 0.034, n = 3); length: mean = 1.51 mm (SD ± 0.134, n = 3); region between the posterior margin of the eyes: mean= 1.98 mm (SD ± 0.038, n = 3); scape, pedicel and flagellum blackish with 32 flagellomeres.

Thorax. Pronotum: width: mean = 1.98 mm (SD ± 0.046, n = 3); length: mean = 0.99 mm (SD ± 0.042, n = 3). Forewing: costal area with nine crossveins; area between M and CuA with two crossveins. Hindwing: similar to forewing; costal area with eight crossveins; MP not bifurcated.

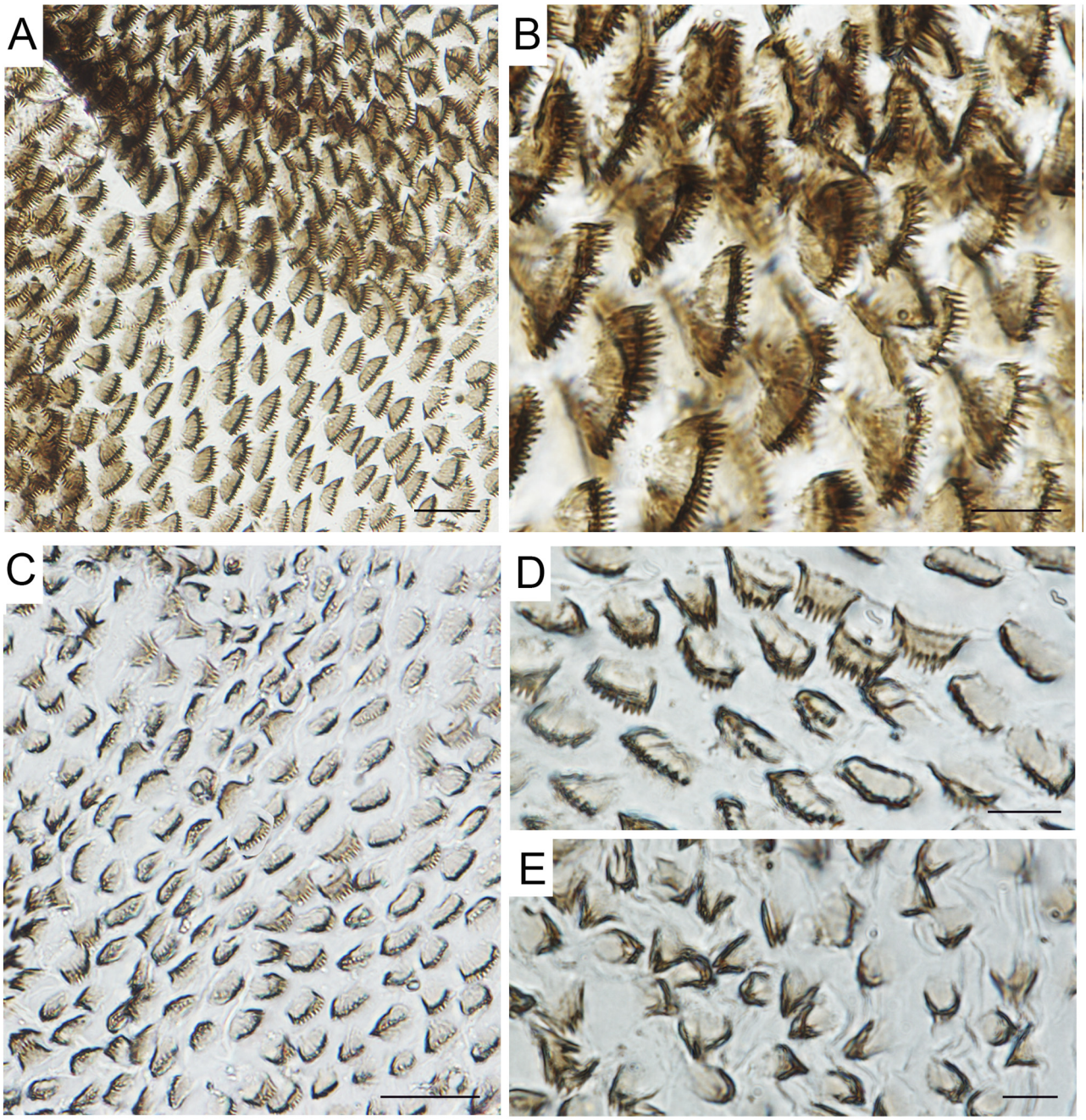

FIGURE 6. *Ilyobius erebus* **sp. nov.**, paratype male genitalia. (A) fringed thorny setae on membranous endophalic sac, general view, (B) same, detail. *Ilyobius hauseri* (Contreras-Ramos, Fiorentin & Urakami, 2005) (Megaloptera: Sialidae), additional specimen collected in the type locality of species, male genitalia. (C) fringed thorny setae on membranous endophalic sac, general view, (D), (E) same, details. Scale bars, A = 0.1 mm; B = 0.01 mm; C = 0.03 mm; D, E = 0.01 mm.

Genitalia (Fig. 7A–E). Sternite 7 with thumb-shaped, posteriorly projected median projection in lateral view (Fig. 7A, B); in ventral view, subtriangular with posterior margin rounded, projected medially (Fig. 7C, D). Tergite 9 subtrapezoidal, in lateral view, ventral region broadly valvate; joined to upper region by junction line (Fig. 7A, B). Gonocoxite 8 reduced, represented by a small, setose sclerite in ventral view (Fig. 7E), located beneath sternite 7 (Fig. 7C, D). Gonapophysis 8 as a single straight sclerotized plate; in lateral view, subrectangular with falcate dorsal apex (Fig. 7A, B); in ventral view, subrectangular in shape, with anterior margin slightly concave and posterior margin convex, with lateral regions falcate (Fig. 7C, D). Gonocoxite 9 subretangular in lateral view, setose, posteriorly with a small gonostylus 9 at apex (Fig. 7A, B). Ectoproct setose, in lateral view, short, ovoid (Fig. 7A, B).

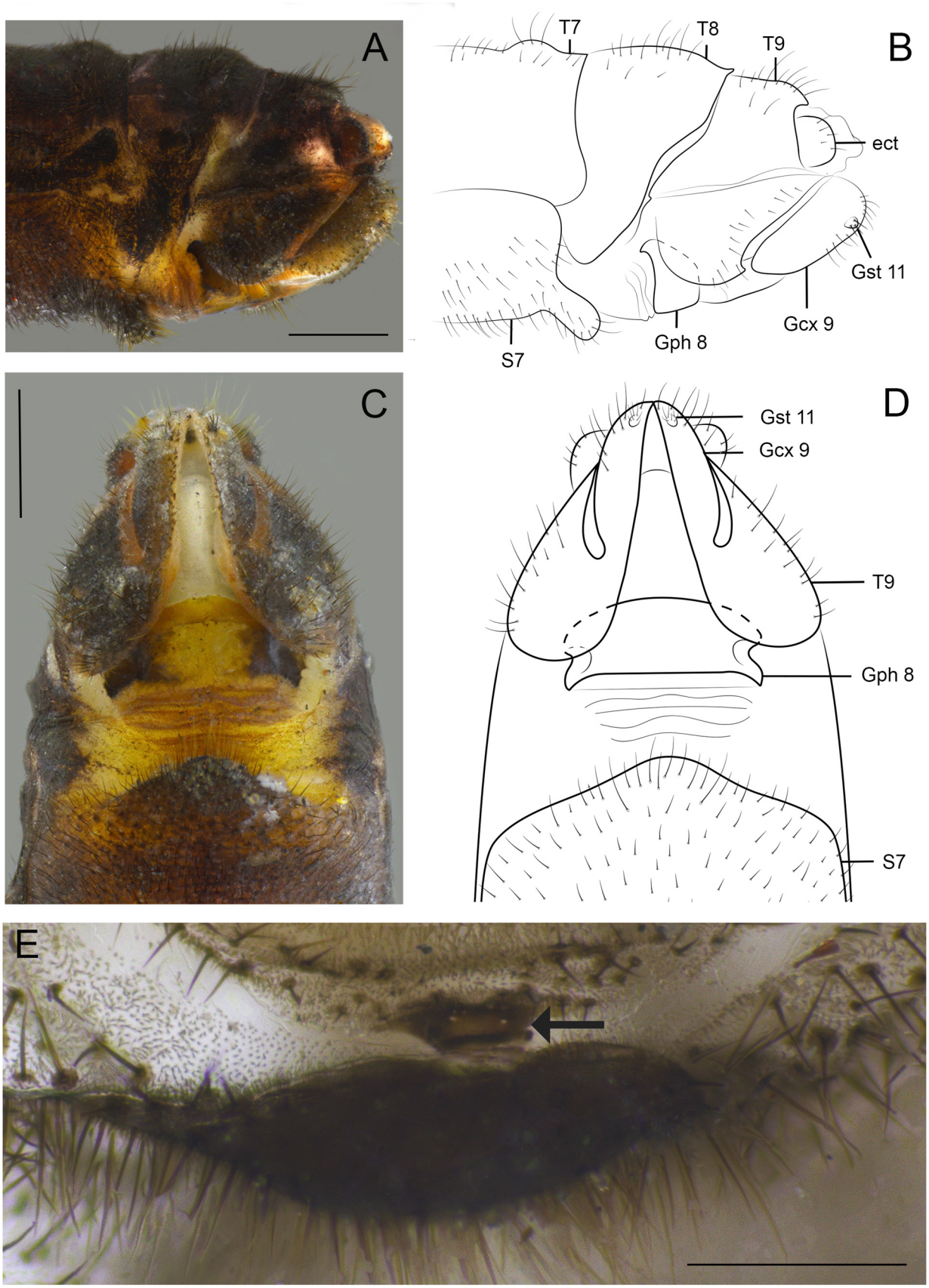

FIGURE 7. *Ilyobius erebus* **sp. nov.**, female. (A) genitalia, lateral; (B) morphological interpretation of genital sclerites in A; (C) genitalia, ventral; (D) morphological interpretation of genital sclerites in C; (E) genitalia, ventral, the arrow indicates the gonocoxite 8 beneath S7. Scale bars, A, C = 0.5 mm, E = 0.2 mm.

FIGURE 8. *Ilyobius erebus* **sp. nov.**, mature larvae. (A) habitus, dorsal; (B) head, lateral; (C) head, dorsal; (D) head, ventral. Scale bars, A= 2 mm; B = 0.5 mm; C, D = 1 mm.

Mature larvae (Fig. 8A–D). Length = 10.24 mm (except caudal filament); maximum width = 2.32 mm (n =1).

Head (Fig. 8B, D). Length, from the clypeal margin to distal region of the head capsule = 2.49 mm; maximum width = 2.36 mm; subquadrate. Orange-brown in color, with darker areas on anterior region (Fig. 8C); strongly sclerotized; muscle scars on posterior half (Fig. 8C); several thin sparse setae distributed on head capsule. Clypeus wide and narrow, length = 0.24 mm; width = 1.72 mm. Antenna (Fig. 9D) 4-articulated; first antennomere longer than wide, wider than the others; second antennomere longer than others, ca. 2.5X longer than antennomere 1;

antennomere 3 slender, ca. 1.5X longer than antennomere 1; antennomere 4 slender and shorter than antennomere 3, apically with short, setiform sensilla. Labrum (Fig. 9A) strongly sclerotized, subtriangular, ca. 5X wider at base than at apex; basally slightly wider than long; lateral margins concave; with thin setae sparsely distributed in dorsal view; in ventral view, with two pointed apophyses at tip. Mandible (Fig. 9C) symmetrical, slender and long, sharply

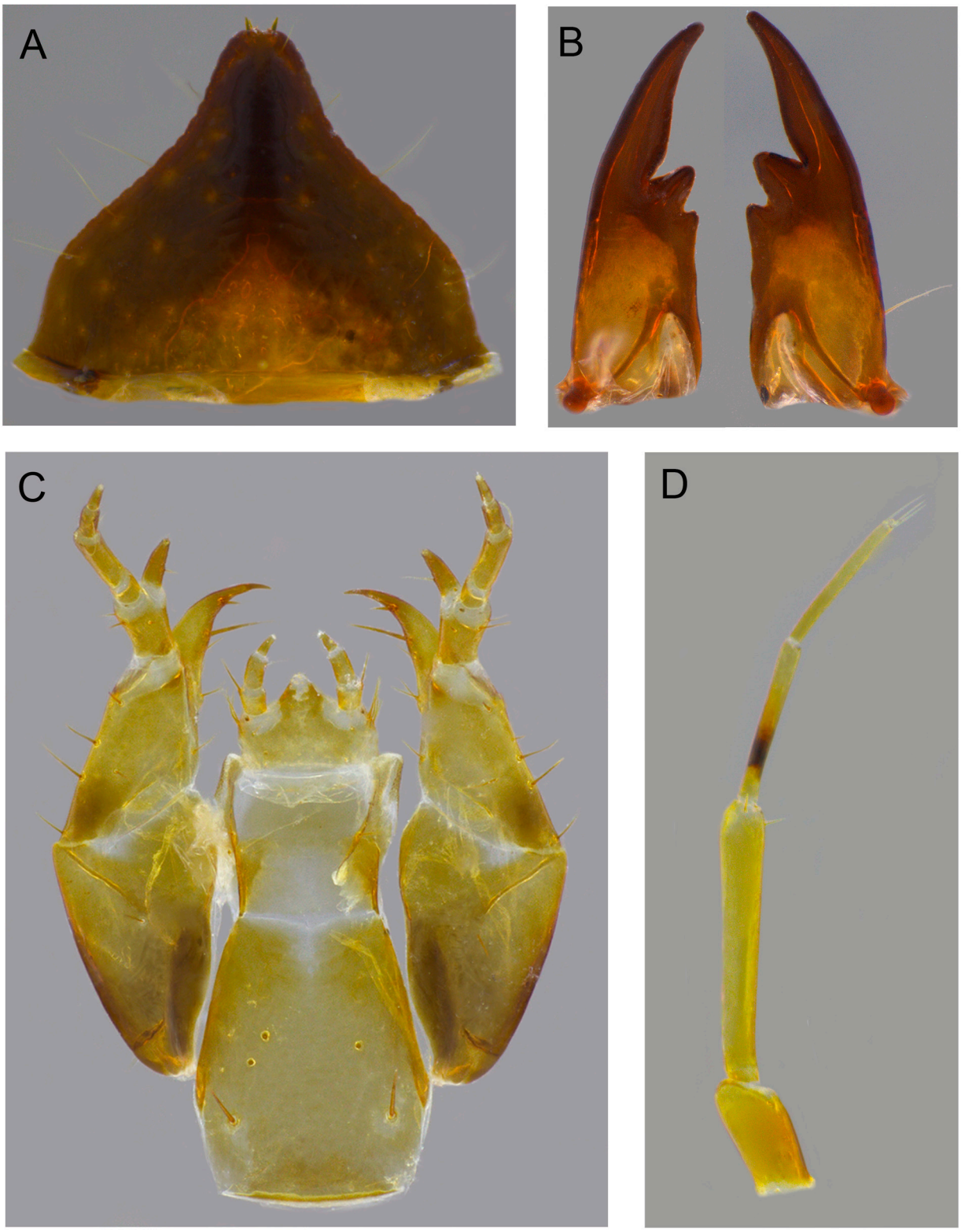

FIGURE 9. *Ilyobius erebus* **sp. nov.**, mature larvae. (A) labrum, dorsal; (B) maxillolabial complex, ventral; (C) mandible, ventral; (D) antenna. Scale bars, A–D = 0.5 mm.

pointed with minute basal tooth (difficult to see in specimens with worn mandibles), with two preapical teeth and a sharp terminal tooth, slightly serrated at base; outer margin convex, with basal, thin, long seta, and short slender seta near midlength. Maxilla (Fig. 9B), in ventral view, with cardo and stipes subtriangular; cardo ca. 1.5X longer than stipes. Lacinia hook-like, well developed. Galea cone-shaped. Palpifer subrectangular. Palpus: first palpomere wider than long, shorter than others; second palpomere longer than others, twice the length of the third; fourth palpomere cone-shaped. Labium (Fig. 9B*)* with submentum hexagonal in ventral view, ca. 1.1X longer than cardo; mentum subrectangular, slightly longer than wide, ca. 1.8X shorter than submentum, with lightly sclerotized areas; prementum wider than long, ca. 1.2X narrower than mentum; with well-developed membranous ligula.

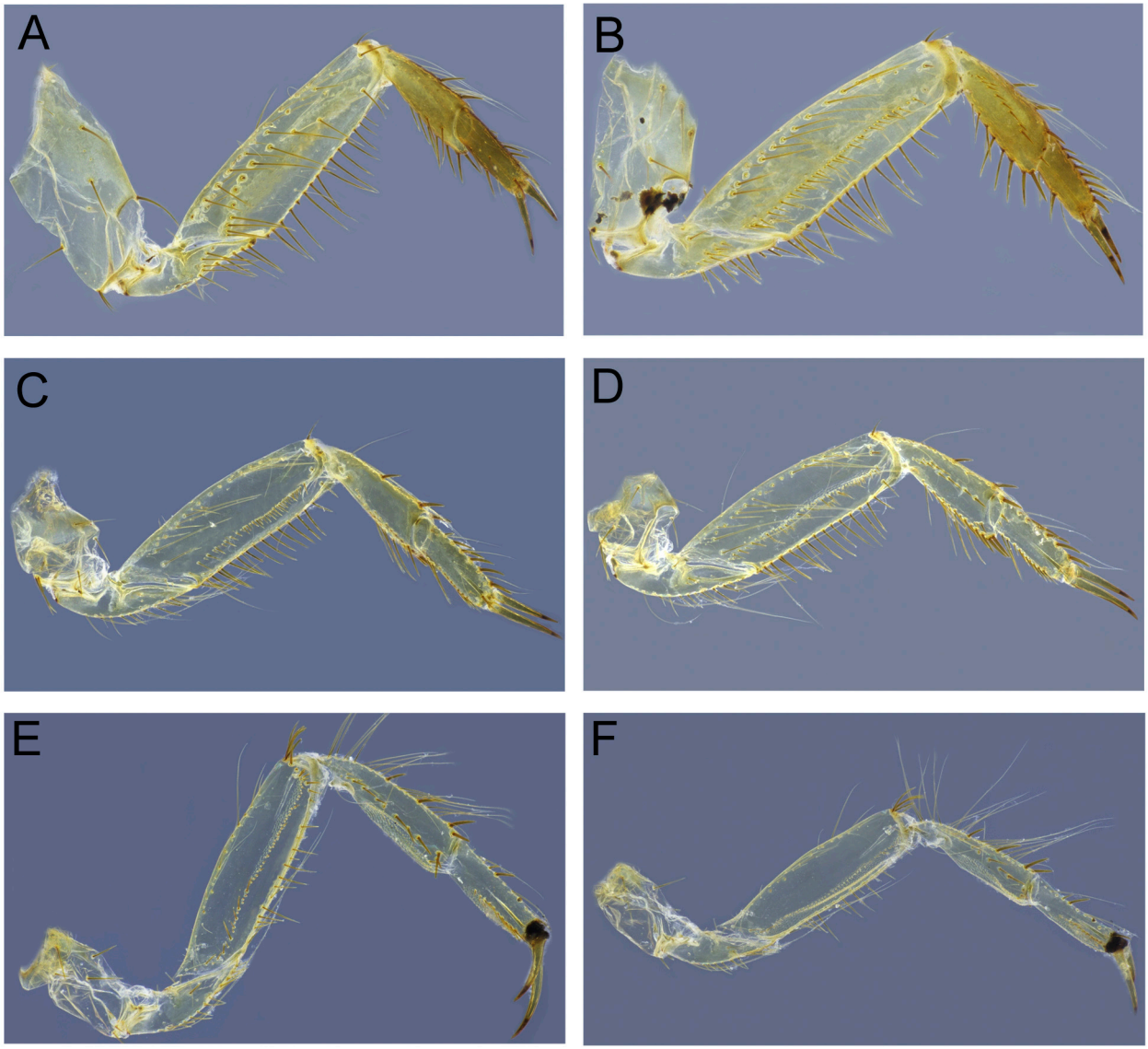

FIGURE 10. *Ilyobius erebus* **sp. nov.**, mature larvae. (A) prothoracic leg, internal; (B) prothoracic leg, external; (C) mesothoracic leg, internal; (D) mesothoracic leg, external; (E) metathoracic leg, external; (F), metathoracic leg, internal. Scale bars = 1 mm.

Thorax (Figs 8A, 10A–C). Tergites orange, with diffuse blackish marks, especially on meso- and metanotum (Fig. 8A). Pronotum: length = 1.61 mm; maximum width = 2.39 mm; subrectangular, anterior margin slightly rounded, posterior margin straight. Legs (Fig. 10A–F): yellowish. Coxa of all legs slightly wider than long, with few setae sparsely distributed (Fig. 10A–F). Profemur ca. 3.5X longer than wide; internal margin with long, thick setae; internal surface with two rows of long setae near external margin (Fig. 10A); external surface with long, thick setae near external margin and with a row of shorter setae on the submedial region (Fig. 10B); mesofemur ca. 3X longer than wide; internal margin with long, thick setae; internal and external surface with a row of long setae near

external margin; internal surface with a row of short setae near internal margin (Fig. 10C); external surface with a row of short setae on submedial region (Fig. 10D); hindfemur ca. 3.5X longer than wide; internal margin with long, thick setae; internal and external surface with a row of long, thin setae near external margin (Fig. 10E, F); external surface with a row of shorter setae on submedial region and with a row of pectinate sensillae above submedial row of setae (Fig. 10E); internal surface with a row of short setae near internal margin with a row of pectinate sensillae between the internal margin and the row of setae on the submedial region (Fig. 10F). Protibia ca. 2.6X longer than wide; mesotibia ca. 2.9X longer than wide; foretibia subequal in size to mesotibia. Tibia of all legs with few, long, thick setae on internal and external margins; with thin, long setae on external margin (Fig. 10A–F); internal margin with a long, thick seta; external surface of pro- and mesothoracic legs with a row of short, thick setae submedially (Fig. 10B, D); external and internal surface of metathoracic leg with pectinate sensillae below the submedial row of setae (Fig. 10E, F). Protarsus ca. 3.5X longer than wide; mesotarsus ca. 3.9X longer than wide; metatarsus ca. 3X longer than wide; internal and external margin of prothoracic and mesothoracic leg with thick setae; external margin with thin setae; external surface with longitudinal row of thick setae dorsally and ventrally (Fig. 10B, D); external and internal surface of metathoracic leg, with a row of short, thick setae submedially; with pectinate sensillae below the submedial row of setae (Fig. 10E, F). Tarsal claws with approximately the same width along the entire length.

Abdomen (Fig. 8A). Poorly sclerotized; light brown; abdominal gills whitish translucent.

Etymology. The specific epithet is derived from *Erebus*, Latin for darkness, an allusion to the coloration of this new species, the first in the genus that is almost completely dark. The name is a genitive in the fourth declension.

Distribution. Poços de Caldas municipality, Morro do Ferro, Minas Gerais State, Brazil (Fig. 1A, B).

Ilyobius hauseri (Contrera-Ramos, Fiorentin & Urakami, 2005)

(Figs 4C–E; 11–12)

Protosialis hauseri Contreras-Ramos *et al*. 2005: 268 (original description); Contreras-Ramos 2008: 808 (taxonomy).
Ilyobius hauseri; Liu *et al*. 2015a: 31 (phylogeny of Sialidae; comb. nov.); Liu *et al*. 2015b: 55 (key of species); Oswald 2018 (online catalog); Ardila-Camacho *et al*. 2021: 48 (taxonomy); Rafael *et al*. 2022 (online catalog).

Material examined. Holotype: male genitalia, Brazil; Rio Grande do Sul, Floresta Nacional de São Francisco de Paula, (29°02'S; 50°23'W, 930 m) 17.VIII.2003 (larva collected) - 20.IX.2003 (adult emerged in laboratory), Y. Urakami & G.L. Fiorentin cols. (MCNZ). Paratype: female genitalia, same data as holotype. **Additional specimens:** same as holotype, except the following data: seven males, three fixed in 80% alcohol, four pinned; three females, two fixed in 80% alcohol, one pinned, 30.VIII.2015 (larva collected)—02.IX.2015 (adult emerged in laboratory), N. Hamada, C. Benetti, G. Dantas, A.M.O. Pes cols. (INPA).

Male genitalia redescription (Figs 6C–E; 11A–D). Tergite 9 sclerotized, sparsely setose; in lateral view, subtriangular with rounded margin (Fig. 11A, B); in dorsal view, sub-rectangular; basal margin concave, distal margin convex. Sternite 9 trifurcate; sparsely setose; central projection slightly longer than lateral ones (Fig. 11B); in lateral view, central projection with similar width along entire length (Fig. 11B). Endophalic sac membranous, eversible, with several fringed thorny setae (Fig. 6C–E). Gonocoxite 9 robust, setose; in lateral view, subtriangular, with rounded apex, dorsal margin slightly convex (Fig. 11A, B). Anal tubercle membranous. Ectoprocts paired, in lateral view, rounded; dorsal margin convex; ventral margin straight, directed downwards with proximal margin fused to gonocoxite 11 (Fig. 11B); in caudal view, subcylindrical (Fig. 11D). Gonocoxite 11, in lateral view, L-shaped, distal region rounded at apex and projected downwards representing gonostylus 11 (Fig. 11B); gonocoxite 11 divided into two sclerites in caudal view, medially directed and connected by a membranous region (Fig. 11D); each sclerite with internal margin straight. Gonostylus 11, in lateral view, distally rounded and projected downwards.

Female genitalia redescription (Fig. 12A–E). Sternite 7 with posteriorly projected, thumb-shaped, posteromedian projection in lateral view (Fig. 12A, B); in ventral view, subpentagonal, with a tubercular projection medially (Fig. 12C, D). Tergite 9 with ventral region broadly valvate in lateral view; joined to upper region by a junction line (Fig. 12A, B). Gonocoxite 8 reduced to small, unpaired, setose sclerite (Fig. 12E), located beneath sternite 7 (Fig. 12C, D). The gonapophyses 8 is present as a single, strongly sclerotized plate; in lateral view, subquadrate, dorsal margin convex proximally, concave distally (Fig. 12A, B); in ventral view, subrectangular in shape, with anterior margin concave medially, posterior margin convex medially, lateral regions enlarged, with a sclerotized fold at the tip of each side (Fig. 12C, D). Gonocoxite 9 subrectangular in lateral view, setose, posteriorly with small gonostylus 9 at apex (Fig. 12A, B). Ectoproct short and ovoid in lateral view, setose (Fig. 12A, B).

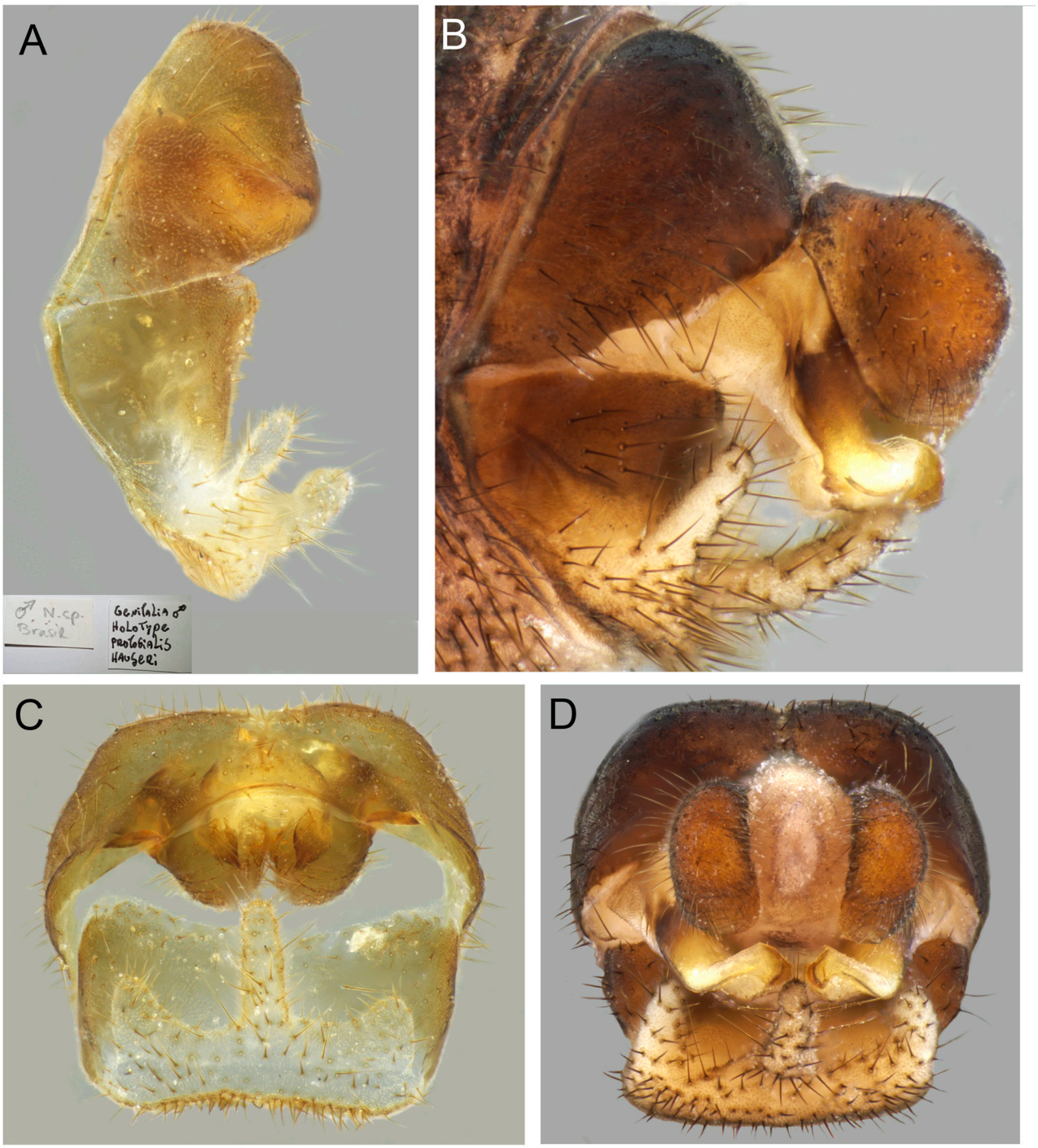

FIGURE 11. *Ilyobius hauseri* (Contreras-Ramos, Fiorentin & Urakami, 2005), male, genitalia. (A), (C) holotype, lateral and caudal, respectively; (B), (D) additional specimen collected in the type locality of the species. Scale bars, A = 0.25 mm; B–D = 0.2 mm.

Remarks. No adults were collected in Malaise and Pennsylvania light traps installed at the stream's banks where the new species larvae were collected. *Ilyobius erebus* **sp. nov.** is closely related to *I. hauseri* based on the morphology of the male and female genitalia, and to *I. nubilus* based on the morphology of the female genitalia. Male genitalia of *I. hauseri* and *I. erebus* **sp. nov.** share the subtriangular tergite 9 with rounded margins, the endophalic sac with several fringed thorny setae, and the trifurcated sternite 9, in which the median protrusion is elongate. In addition, the male gonocoxite 9 is subtriangular with rounded margins, and the ectoprocts have basal margin fused to gonocoxite 11 in both species. The L-shaped gonocoxite 11 constitutes a common characteristic of these two species.

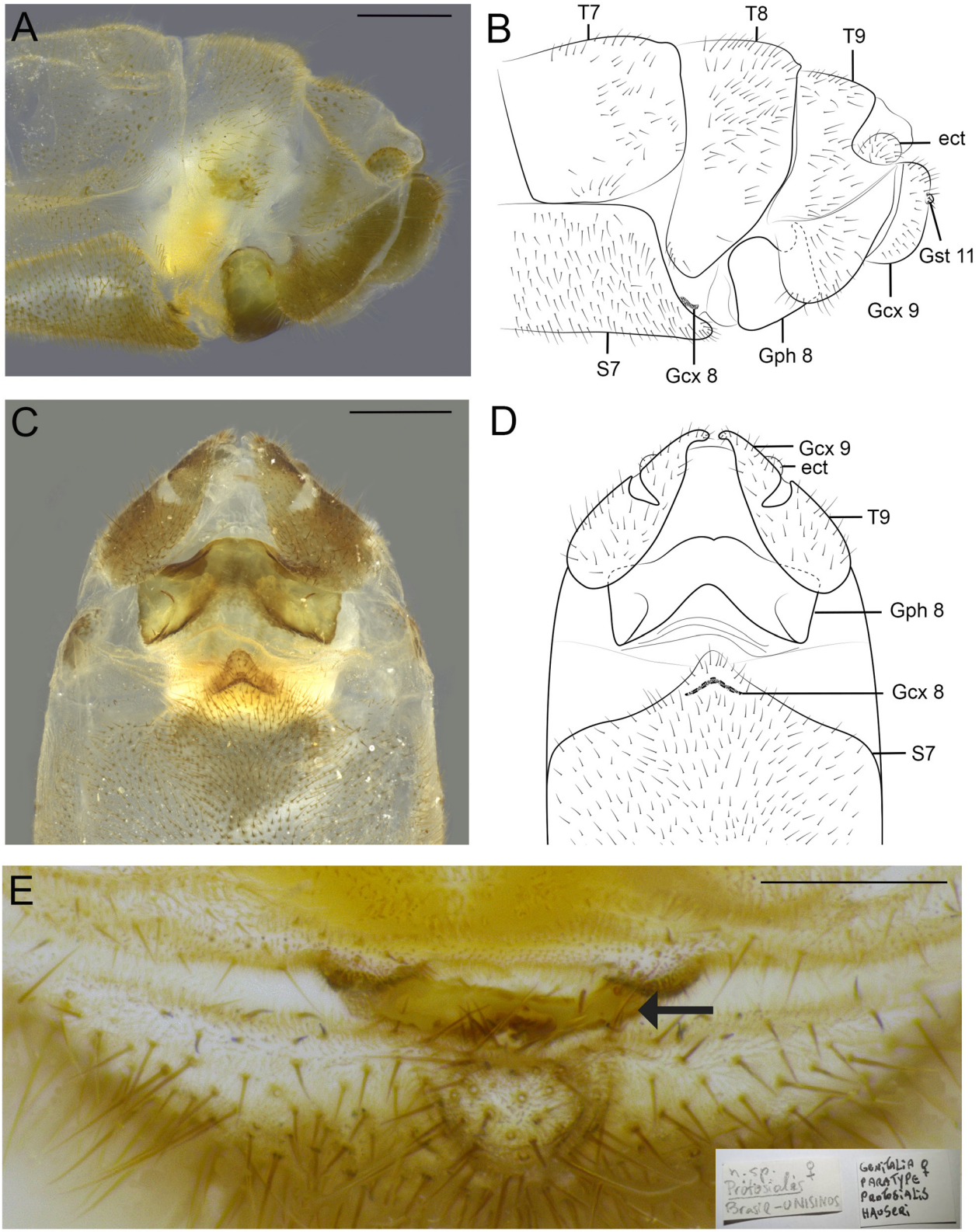

FIGURE 12. *Ilyobius hauseri* (Contreras-Ramos, Fiorentin & Urakami, 2005), genitalia of female paratype. (A) lateral; (B) morphological interpretation of genital sclerites in A; (C) ventral; (D) morphological interpretation of genital sclerites in C; (E) ventral, the arrow indicates the gonocoxite 8 underneath S7. Scale bars, A, C = 0.5 mm, E = 0.2 mm.

The female genitalia of *I. erebus* **sp. nov.**, *I. hauseri* and *I. nubilus* have gonocoxite 8 reduced, representing a tiny, setose sclerite, located beneath sternite 7 (Figs 7E, 11E), while the two gonapophyse 8s form a single sclerotized plate (Contreras-Ramos *et al*. 2005, Contreras-Ramos 2008, Liu *et al*. 2015a). However, the new species can be easily differentiated from *I. hauseri* and *I. nubilus* based on the following characters: in *Ilyobius erebus* **sp. nov.** the head is almost completely blackish, while in *I. hauseri* it is orange, with median, longitudinal, black band. The head in *I. nubilus* is black, slightly paler around the epicranial suture (Contreras-Ramos 2008). Although these three species share the dark pronotum, *I. hauseri* has orangish-brown areas, which are absent in *I. erebus* **sp. nov.** and *I. nubilus*. In *I. erebus* **sp. nov.**, the sternite 9 has the median projection wider medially (Fig. 4A, B), while it has the same width along its entire length in *I. hauseri* (Fig. 11B). Gonostylus 11 projects upwards distally in *I. erebus* **sp. nov.** (Fig. 4A, B), whereas in *I. hauseri* it is distally projecting downwards (Fig. 11B). The ectoprocts are subrectangular in dorsal view in *I. hauseri*, and the ventral margin is directed downwards in lateral view. By contrast, the ectoprocts are subtriangular, and the ventral margin is posteriorly directed in ventral view in *I. erebus* **sp. nov.** The female genitalia of *I. hauseri*, have gonapophysis 8 dorsally curved, with posterior margin strongly convex (Contreras-Ramos *et al*. 2005), however, this structure is ventrally depressed and widened on the posterior half, with a broadly arched posterior incision in *I. nubilus* (Contreras-Ramos 2008). In *I. erebus* **sp. nov.**, the two gonapophysis 8 appear as a single and straight sclerotized plate with anterior and posterior margins slightly convex, and the anterolateral corners are falcate (Fig. 7C, D).

The larvae of *Ilyobius erebus* **sp. nov.** can be easily differentiated from *I. chilensis* (McLachlan, 1870) by the distinct general coloration of head and pronotum: the larva of *I. chilensis* has a distinct pattern of dark brown marks on the head, which are absent in the new species (Fig. 8C) (Archangelsky *et al*. 2017). Liu *et al*. (2015a) divided *Ilyobius* into two species groups (the *I. chilensis* group, and the *I. mexicanus* group). The first group is composed of *I. chilensis, I. hauseri* and *I. nubilus,* while the remaining species of *Ilyobius*, i.e., *I. bimaculatus* (Banks, 1920), *I. curvatus* (Liu, Hayashi & Yang, 2015), *I. flammatus*, *I. flavicollis*, *I. mexicanus* (Banks, 1901), *I. nigrocephalus* Ardila-Camacho, Martins & Contreras-Ramos, 2021, and *I. ranchograndis* (Contreras-Ramos, 2006) belong to the second group (Liu *et al*. 2015a; Ardila-Camacho *et al*. 2021). *Ilyobius erebus* **sp. nov.** is placed in the *I. chilensis* group based on the morphology of the male sternite 9, which has an elongate median protrusion, the transversely band-like male gonocoxite 11 with short median processes, and the reduced female gonocoxite 8 (Liu *et al*. 2015a).

Conservation. Land-use change is one of the main threats driving the decline in freshwater environments (Sala *et al*. 2000). The natural vegetation in the region of the type locality of *I. erebus* **sp. nov.** has been replaced by *Eucalyptus* plantations; this fact directly and indirectly affects the aquatic biota through soil disturbance, which changes the limnological conditions (Pozo *et al*. 1997). *Eucalyptus* leaves contain tannins and phenols that can change the chemical composition of water, reduce dissolved nutrients, and consequently prevent the colonization of organic matter by the decomposing microbiota (Pozo *et al*. 1997).

The integrity and heterogeneity of the environment is a fundamental factor for colonization and permanence of aquatic insects (Santos *et al*. 2020). Frequent and intense environmental impacts on these ecosystems can eliminate communities, especially in the case of species that have biological traits that disfavor more-active dispersive processes (Poff *et al*. 2006). *Ilyobius* is a rare taxon with few occurrence points and weak dispersion (Penny 1981, Contreras-Ramos 2008); therefore, the new species may be subject to habitat loss in the Morro do Ferro region.

Conclusions

Ilyobius erebus **sp. nov.** is the fourth species of genus recorded for Brazil and the total number of *Ilyobius* species increases to 11. The *I. erebus* **sp. nov.** larva is the second that has been formally described for the genus, and its description includes more detailed characters of taxonomic relevance, providing information needed for future larval descriptions. We highlight that the new species was found in a locality affected by land-use change, and its permanence may therefore be threatened.

Acknowledgments

Financial and infrastructure support was provided to NH by MCTI/CNPq/MEC/CAPES/PROTAX (440616/2015-8); CAPES, Proequipamentos and Finance Code 001—PPG Entomologia; INCT ADAPTA II funded by CNPq (465540/2014-7), FAPEAM (062.1187/2017); FAPEAM—Programa POSGRAD and MCTI/ INPA. We thank IBAMA (Brazilian Institute of Environment and Renewable Natural Resources) for collection permissions. NH is a CNPq research fellow (308970/2019-5), GCM received a M.Sc. fellowship from FAPEAM, JMCN received a fellowship from CAPES (88887.313046/2019-00) and the PCI Program (MTCI/ CNPq/ INPA). Several people collaborated in the fieldwork, including E. H. Ferreira, J. O. Silva, I. F. Rossi, R Heldt Jr and T. T. S. Polizei. We thank V. P. Ramos and the farm owner for permission to collect on his land. We thank Drs. Atilano Contreras-Ramos (UNAM) and Caleb C. Martins for sending and bringing, respectively, the types of *I. hauseri* to Brazil. P.M. Fearnside reviewed the English grammar.

References

Ardila-Camacho, A., Rivera-Gasperín, S.L., Martins, C.C. & Contreras-Ramos, A. (2021) A reappraisal of the taxonomy of Neotropical Sialidae (Insecta: Megaloptera): with the description of a new genus from Cuba. *European Journal of Taxonomy*, 782, 21–54.
https://doi.org/10.5852/ejt.2021.782.1587

Archangelsky, M., Pessacq, P. & Berrondo, M. (2017) Description of the larva of *Ilyobius chilensis* (McLachlan) (Megaloptera: Sialidae) and notes on the adult morphology. *Zootaxa*, 4318 (1), 177–186.
https://doi.org/10.11646/zootaxa.4318.1.10

Beutel, R.G. & Friedrich, F. (2008) Comparative study of larval head structures of Megaloptera (Hexapoda). *European Journal of Entomology*, 105, 917–938.
https://doi.org/10.14411/eje2008.119

Borges, M.G., Leite, M.E. & Leite, M.R. (2018) Mapeamento do eucalipto no estado de Minas Gerais utilizando o Sensor Modis. *Espaço Aberto*, 8, 53–70.
https://doi.org/10.36403/espacoaberto.2018.14364

Breitkreuz, L.C., Winterton, S.L. & Engel, M.S. (2017) Wing tracheation in Chrysopidae and other Neuropterida (Insecta): A resolution of the confusion about vein fusion. *American Museum Novitates*, 2017, 1–44.
https://doi.org/10.1206/3890.1

Chapman, N.A., McKinley, I.G., Shea, M.E. & Smellie, J.A.T. (1991) *The Poços de Caldas Project: Summary and implications for radioactive waste management (No. NAGRA-NTB—90-33). Nationale Genossenschaft fuer die Lagerung Radioaktiver Abfaelle (NAGRA)*. Available from: https://www.skb.com/publication/7708/TR90-24_inlaga.pdf (accessed 4 July 2022)

Contreras-Ramos, A., Fiorentin, G.L. & Urakami, Y. (2005) A new species of alderfly (Megaloptera: Sialidae) from Rio Grande do Sul, Brazil. *Amazoniana*, 18, 267–272.

Contreras-Ramos, A. (2008). Notes on some Neotropical alderflies (Sialidae: Megaloptera). *Annals of the Entomological Society of America*, 101, 808–814.
https://doi.org/10.1093/aesa/101.5.808

Kawada, R. & Buffington, M.L. (2016) A scalable and modular dome illumination system for scientific microphotography on a budget. *PLoS One*, 11, e0153426.
https://doi.org/10.1371/journal.pone.0153426

Liu, X., Hayashi, F. & Yang, D. (2015a) Phylogeny of the family Sialidae (Insecta: Megaloptera) inferred from morphological data, with implications for generic classification and historical biogeography. *Cladistics*, 31, 18–49.
https://doi.org/10.1111/cla.12071

Liu, X., Hayashi, F. & Yang, D. (2015b) Taxonomic notes of the Neotropical alderfly genus *Ilyobius* Enderlein, 1910 (Megaloptera, Sialidae), with description of a new species. *Deutsche Entomologische Zeitschrift*, 62, 55.
https://doi.org/10.3897/dez.62.4481

Liu, X., Lü, Y., Aspöck, H., Yang, D. & Aspöck, U. (2016) Homology of the genital sclerites of Megaloptera (Insecta: Neuropterida) and their phylogenetic relevance. *Systematic Entomology*, 41, 256–286.
https://doi.org/10.1111/syen.12154

New, T.R. & Theischinger, G. (1993) Megaloptera, Alderflies and Dobsonflies. *Handbuch der Zoologie*, 4 (Arthropoda: Insecta), Part 33, 1–97.

Oswald, J.D. (2018) Neuropterida Species of the World. Version 5.0. Available from: http://lacewing.tamu.edu/SpeciesCatalog/Main (accessed 15 January 2022)

Penny, N.D. (1981) Neuroptera of the Amazon Basin. Part 4. Sialidae. *Acta Amazonica*, 11, 843–846.
https://doi.org/10.1590/1809-43921981114843

Poff, N.L., Olden, J.D., Vieira, N.K., Finn, D.S., Simmons, M.P. & Kondratieff, B.C. (2006) Functional trait niches of North

American lotic insects: traits-based ecological applications in light of phylogenetic relationships. *Journal of the North American Benthological Society*, 25, 730–755.
https://doi.org/10.1899/0887-3593(2006)025[0730:FTNONA]2.0.CO;2

Pozo, J., González, E., Díez, J.R., Molinero, J. & Elósegui, A. (1997) Inputs of particulate organic matter to streams with different riparian vegetation. *Journal of the North American Benthological Society*, 16, 602–611.
https://doi.org/102307/1468147

Rafael, J.A., Câmara, J.T. & Heleodoro, R.A. (2022) Sialidae in Catálogo Taxonômico da Fauna do Brasil. PNUD. Available from: http://fauna.jbrj.gov.br/fauna/faunadobrasil/65481 (accessed 24 February 2022)

Sala, O.E., Chapin, F.S., Armesto, J.J., Berlow, E., Bloomfield, J., Dirzo, R., Huber-Sanwald, E., Huenneke, L.F., Jackson, R.B., Kinzig, A., Leemans, R., Lodge, D.M., Mooney, H.A., Oetserheld, M., Poff, N.L., Sykes, M.T., Walker, B.H., Walker, M & Wall, D.H. (2000) Global biodiversity scenarios for the year 2100. *Science*, 287, 1770–1774.
https://doi.org/10.1126/science.287.5459.1770

Santos, M.R.D., Saito, V.S., Pamplin, P.A.Z., Pereira, A.A. & Fonseca-Gessner, A.A. (2020) Pollution tolerance, flight capacity and natural history explain metacommunity structure in high-altitude stream insects. *Acta Limnologica Brasiliensia*, 32. [published online]
https://doi.org/10.1590/s2179-975x1019

Sardinha, D.D.S., Pena, Y.T.L., Tiezzi, R.D.O. & Almeida, M.C.J.D. (2016) Data base of natural disasters in Poços de Caldas: A tool for land planning and management. *Revista Brasileira de Gestão Urbana*, 8, 318–331.
https://doi.org/10.1590/2175-3369.008.003.AO03